

Quasiparticle Freeze-Out in Superconducting Tunnel Junction X-ray Detectors with Killed Base Electrode

**V. A. Andrianov, L. V. Filippenko &
S. Friedrich**

Journal of Low Temperature Physics

ISSN 0022-2291

Volume 176

Combined 3-4

J Low Temp Phys (2014) 176:584–590
DOI 10.1007/s10909-013-1016-1

Volume 176 • Numbers 3/4 • August 2014

**Journal of
Low Temperature
Physics**

Special Issue: Low Temperature Detectors (LTD-15), Part I

10909 • ISSN 0022-2291
176(3/4) 131–616 (2014)

 Springer

 Springer

Your article is protected by copyright and all rights are held exclusively by Springer Science +Business Media New York. This e-offprint is for personal use only and shall not be self-archived in electronic repositories. If you wish to self-archive your article, please use the accepted manuscript version for posting on your own website. You may further deposit the accepted manuscript version in any repository, provided it is only made publicly available 12 months after official publication or later and provided acknowledgement is given to the original source of publication and a link is inserted to the published article on Springer's website. The link must be accompanied by the following text: "The final publication is available at link.springer.com".

Quasiparticle Freeze-Out in Superconducting Tunnel Junction X-ray Detectors with Killed Base Electrode

V. A. Andrianov · L. V. Filippenko · S. Friedrich

Received: 15 July 2013 / Accepted: 9 December 2013 / Published online: 23 January 2014
© Springer Science+Business Media New York 2014

Abstract The current–voltage characteristics of superconducting tunnel junction (STJ) X-ray detectors were measured in the temperature range from 4.2 to 0.1 K. The freeze-out of the thermal tunneling current was compared between an STJ detector with a traditional Nb/Al/Al₂O₃/Al/Nb layer structure and a Ti/Nb/Al/Al₂O₃/Al/Nb/NbN detector whose low-gap Ti film kills the X-ray response of the base electrode. The current decrease and the linear low-temperature I(V) characteristics for the detector with the killed electrode can be qualitatively explained by tunneling current contributions from the subgap states of the Ti film. The data are analyzed on the basis of the proximity theory in the dirty limit.

Keywords X-rays detectors · Superconducting tunnel junctions · Quasiparticles · Proximity theory · Density of states

1 Introduction

Superconducting tunnel junctions (STJs) are being developed as single photon detectors because of their excellent energy resolution, high speed and low energy threshold of registration [1]. At 5.9 keV, their energy resolution of ∼10–20 eV is substan-

V. A. Andrianov
Skobeltsyn Institute of Nuclear Physics, Lomonosov Moscow State University, 119991 Moscow,
Russian Federation

L. V. Filippenko
Institute of Radio Engineering and Electronics RAS, 103907 Moscow, Russian Federation

S. Friedrich (✉)
Lawrence Livermore National Laboratory, Livermore, CA 94550, USA
e-mail: friedrich1@llnl.gov

tially better than the 140–150 eV resolution of typical silicon detectors. In the optical range, they offer photon-counting capability with an energy resolution of about 10 %. STJ detectors typically employ multilayer electrodes of superconductors with different transition temperatures T_c and different superconducting gaps Δ to increase the tunneling probability for excess quasiparticles and enable charge multiplication by backtunneling [2]. Traditionally, Nb/Al bilayer electrodes have been used to form symmetric Nb/Al/AlO_x/Al/Nb STJ detectors, with the thick Nb-layer ($T_c \approx 9$ K) serving as the X-ray absorber and the thin Al-layer ($T_c \approx 1.2$ K) near the tunnel barrier as a quasiparticle trap. These devices have achieved high energy resolution and higher speed than most other cryogenic detectors, but suffer from a line splitting artifact due to the difference of the signals from photon absorption in the top and bottom electrodes.

An alternative STJ detector design uses a low-gap film to suppress (“kill”) the X-ray response of the STJ base electrode [3,4]. We have implemented this design by depositing a low-gap Ti trapping layer ($T_c \approx 0.06$ K) below the Nb/Al base electrode to ensure quick absorption of the excess quasiparticles created by X-ray absorption in the base Nb film. In addition, we have deposited a NbN reflection layer on top of the Nb/Al absorber electrode to prevent Nb oxidation and the associated quasiparticle loss at the STJ surface. This detector type not only removes the line splitting artifact, but also speeds up the signal response to ~ 0.2 μ s [4].

We have investigated the effect of the low-gap Ti base layer on the superconducting gap and the density of states in the base electrode. For this we have compared the temperature changes of the current–voltage characteristics for STJ detectors with and without the Ti base layer. We find that the Ti film affects the density of states throughout the base electrode, and discuss this qualitatively on the basis of the proximity theory in the dirty limit. This causes the subgap current to decrease more slowly at low temperatures than expected from the BCS theory, and may affect the electronic noise in STJ X-ray detectors.

2 Experiment

The STJ detectors were fabricated by magnetron sputtering on a Si-substrate with a buffer layer of amorphous AlO_x. Five rhombus-shaped STJ detectors with a 2:1 ratio of the diagonals and areas $S = 400, 400, 1600, 6400$, and $20000 \mu\text{m}^2$, were arranged on one chip. The films had the polycrystalline structure with grains sizes of ~ 10 nm. The tunnel junctions had a normal resistivity of $R_{NS} \approx 400 \Omega\mu\text{m}^2$. Current leads made from Nb were attached to the larger angles of rhombus and had the width of 5–10 μm . Details of detector preparation are given in [4].

Two types of STJ detectors were prepared: A-type detectors had the traditional Nb(200)/Al(4)/AlO_x/Al(10)/Nb(120nm) structure, with thicknesses in nm starting at the substrate. B-type detectors had an additional Ti-layer below and a NbN passivation layer on top to form Ti(30)/Nb(150)/Al(4),AlO_x/Al(12)/Nb(200)/NbN(30nm).

I(V) characteristics of A- and B-type STJs were measured in the temperature range from 4.2 to 1.25 K in a pumped-helium cryostat at the Lomonosov Moscow State University, using a preamplifier with a dc current bias. I(V) curves of B-type STJs were measured at $T = 0.1$ K in an adiabatic demagnetization refrigerator at Lawrence

Livermore National Laboratory, using a preamplifier with a dc voltage bias. In each case, the dc Josephson current was suppressed by an external magnetic field along the short diagonal of the devices.

3 Results and Discussion

Figures 1 and 2 show the quasiparticle branch of the I(V) curves at different temperatures for A- and B-type STJs. At 4.2 K the I(V) curves exhibit typical hysteresis, caused by the gap difference in the base and the top electrodes. For A-type STJs, $\Delta_{\text{base}} - \Delta_{\text{top}} = 0.33$ meV, $\Delta_{\text{base}} = 1.33$ mV and $\Delta_{\text{top}} = 1.0$ mV; and for B-type STJs with the Ti base layer $\Delta_{\text{base}} - \Delta_{\text{top}} = 0.38$ meV, $\Delta_{\text{base}} = 1.34$ mV and $\Delta_{\text{top}} = 0.96$ mV. The Nb gap is slightly reduced from its bulk value due to the proximity effect with the Al films [2,5], and no effect of the Ti trap is observed.

At temperatures below ~ 2 K, where the thermal quasiparticle current has decreased significantly, the I(V) curves show a sharp increase of the current at voltages above Δ/e (Figs. 1b, 2b). This contribution is caused by multiple-particle tunneling and Andreev reflection, is essentially independent of temperature, and depends on the uniformity of the insulating barrier [6].

Fig. 1 I(V) characteristics of A-type Nb/Al/AlO_x/Al/Nb STJs at 4.2 K (a) and 1.25 K (b, c)
(Color figure online)

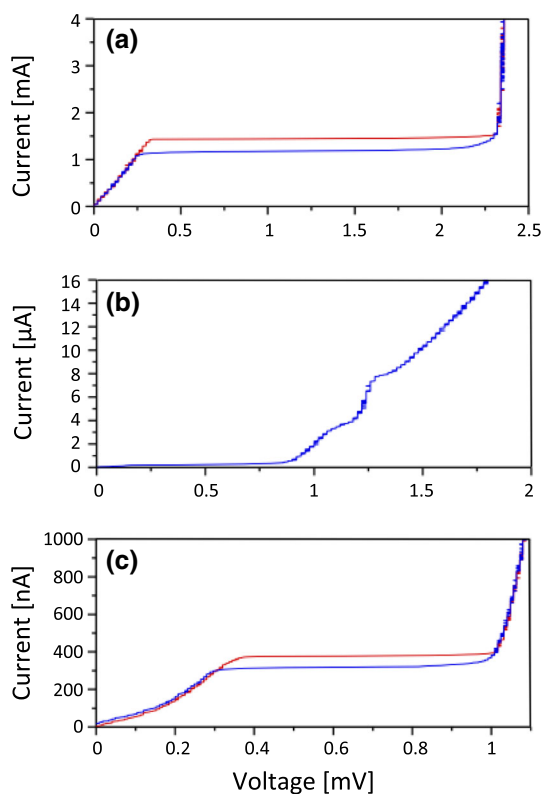
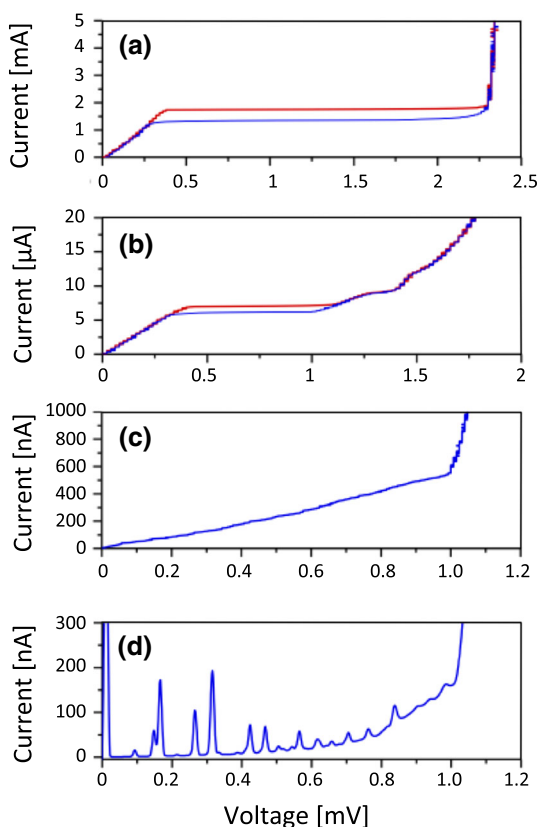


Fig. 2 I(V) characteristics of B-type Ti/Nb/Al_xAlO_x/Al/Nb/NbN STJs at 4.2 K (a), 1.76 K (b), 1.25 K (c) and 0.1 K (d) (Color figure online)

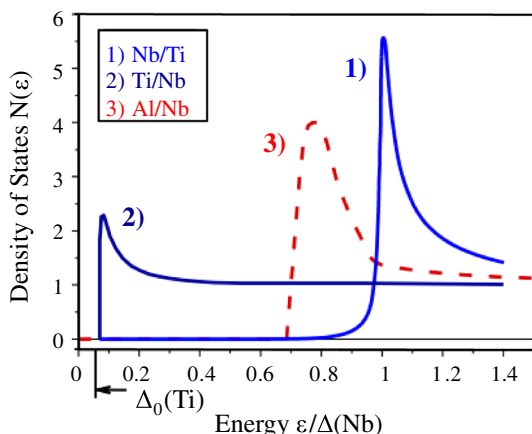


At lower temperatures, A- and B-type STJs behave slightly differently in the voltage range between 0 and Δ/e that is most important for STJ detector operation. In A-type STJs, the decrease in quasiparticle current with temperature follows the BCS model, with a typical hysteresis at $T = 1.25$ K due to single quasiparticle tunneling in an asymmetric junction (Fig. 1c). On the other hand, B-type STJ detectors with the Ti underlayer have no hysteresis at $T = 1.25$ K, and show a resistor-like linear current for $V < \Delta/e$ instead (Fig. 2c). This linear current continues to decrease with temperature until $T \approx 0.1$ K (Fig. 2d, with peaks due to Fiske mode resonances that cannot be fully suppressed by the external magnetic field [7]).

One possible explanation for the observed quasiparticle currents in B-type STJs is the effect of the Ti-trap on the base electrode. In a simple model of Nb/Ti base electrode, the superconducting gap near the tunnel barrier is determined mostly by the Nb layer ($\Delta_{Nb} \approx 1.3$ meV), and the gap near the substrate is determined by the Ti-layer ($\Delta_{Ti} = 0.06$ meV). In this model the Ti layer cannot influence the tunneling current, as the current is determined only by the quasiparticle density of states near the insulating barrier.

However, a proper description of the Nb/Ti base electrode should be based on the proximity theory in the dirty limit [5, 8]. In this case the superconducting gap,

Fig. 3 Density of quasiparticle states, $N(\varepsilon, z)$, in the Ti/Nb/Al_x/Al/Nb/NbN detector: (1) in the base Ti/Nb/Al electrode in Al film close to the tunnel barrier at $z=0$; (2) at the bottom of the Ti film at $z=-(d_{Nb}+d_{Ti})$; (3) in the top Al/Nb/NbN electrode in Al film. Curves (1) and (3) determine the I(V) curve of the STJ (Color figure online)

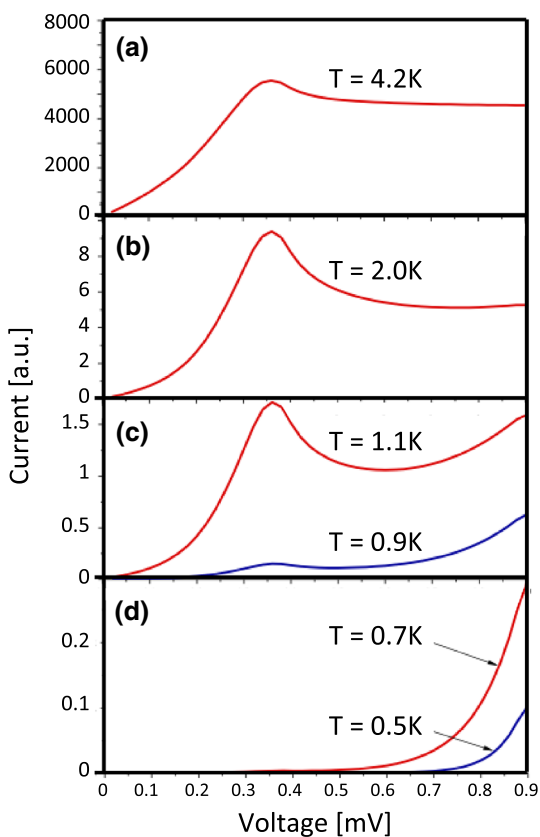


i.e. the lowest possible energy for quasiparticle excitations, is constant for all layers in a multilayer electrode, while the density of states $N(\varepsilon, z)$ strongly depends on the coordinate z perpendicular to the junction plane [8]. In the Nb film close to the tunnel barrier at $N(\varepsilon, z = 0)$, the density of states (DOS) is mostly determined by Nb, but the base electrode will contain additional states at lower energies all the way down to the gap in the Ti trap, although the density of these low-energy states will be much lower.

Curve 1 in Fig. 3 shows the DOS calculated in [9, 10] for a superconductor S/normal metal N sandwich at the outer side of S for the case of $d_S/\xi_S = 10$ where d_S is the thickness and ξ_S is the coherence length in S layer. For our devices we have scaled curve 7 in Fig. 1b of reference [9, 10] by setting the maximum of $N(\varepsilon)$ to 1.36 meV (typical for our Nb films), and setting the edge of the low energy tail to 0.1 meV, since the gap of Ti is enhanced by the proximity effect with Nb. This adaptation qualitatively describes our Ti/Nb/Al electrode near tunnel barrier. The peak density of states at $\varepsilon = \Delta_{Nb}$ corresponds to the unperturbed Nb. In addition, there is a tail in $N(\varepsilon)$ at lower energies due to the states in Ti trap that extends down to the common superconducting energy gap. This low-energy tail in the density of states affects the tunneling current in STJs with a Ti base film at low temperatures. Curve 2 in Fig. 3 shows the expected DOS at the bottom of the Ti-layer. For the top Al/Nb/NbN electrode, we took the typical DOS for a proximity structure with the gap of 0.96 meV from reference [5]. Curve 3 shows $N(\varepsilon, z=0)$ in the Al layer of the top Al/Nb/NbN electrode at the tunnel barrier. Curves 1 and 3 determine the tunneling current of STJ.

Figure 4 shows the calculated I(V) curves at different temperatures, using the standard integrals for STJs [11] and assuming densities of states at the tunnel barrier according to Fig. 3. In these calculations, the top electrode had an energy gap $\Delta_{top}=0.96$ meV (curve 3 in Fig. 3), and the base electrode had a maximum in the density of states at $\varepsilon = 1.36$ meV and a tail in $N(\varepsilon)$ down to a common gap of $\Delta_{base} = 0.1$ meV (curve 1 in Fig. 3). Figure 4c shows a sharp decrease of the maximum current at $V = 0.4$ meV for temperatures between 1.1 and 0.9 K. This causes the reduction of the hysteresis in the experimental I(V) curves. At lower temperatures (Fig. 4d), the calculated I(V) increases monotonically (Fig. 4d), similar to the experimental data at $T = 0.1$ K. Thus,

Fig. 4 Calculations of $I(V)$ curves at various temperatures. For the top electrode $\Delta_{\text{top}}=0.96$ meV, and for the killed electrode the maximum of $N(\varepsilon)$ is at $\varepsilon = 1.36$ meV and the edge of the low energy tail is at $\varepsilon=0.1$ meV (Color figure online)



our calculations confirm the experimental data on a qualitative level. Since the tail in the DOS at low energies is determined by the ratio of Nb thickness d_{Nb} to the coherence length ξ_{Nb} [9, 10], the linear contribution to the tunneling current can likely be reduced by using a thicker Nb base layer.

4 Conclusion

While the addition of a low-gap film at the bottom of an STJ X-ray detector can remove the line splitting artifact and speed up the STJ response, it also introduces undesirable low-energy quasiparticle states at the tunnel barrier. This leads to a slower decrease of the quasiparticle current with temperature than expected from BCS theory alone, and can increase the electronic noise due to the associated decrease in the dynamic resistance. In addition, quasiparticles captured in the low-gap film should have a non-zero probability for tunneling. This may slow down the detector response and lead to additional line broadening at low temperatures when the quasiparticle recombination in the low-gap layer becomes slow [12]. Since this tunneling probability can likely be

reduced by using a thicker Nb base layer, these effect do not fundamentally preclude the fabrication of very fast STJ X-ray detectors with high energy resolution.

References

1. P. Lerch, A. Zender, Quantum Giaever detectors in cryogenic particle detectors, in *Topics in Applied Physics*, 99th edn., ed. by C. Enss (Springer, Berlin, 2005), pp. 217–265
2. N.E. Booth, Appl. Phys. Lett. **50**, 293 (1987)
3. O.J. Luiten, M.L. Van den Berg, J. Gomez Rivas, M.P. Bruijn, F.B. Kiewiet, P.A.J. de Korte, in Proc. of 7th Intern. Workshop on Low Temperature Detectors, ed. by S. Cooper. Munich (1997), p. 25.
4. V.A. Andrianov, L.V. Filippenko, V.P. Gorkov, V.P. Koshelets, Nucl. Instr. Methods A **559**, 683 (2006)
5. A.A. Golubov, E.P. Houwman, J.G. Gijsbertsen, V.M. Krasnov, J. Flokstra, H. Rogalla, M.Y. Kupriyanov, Phys. Rev. B **51**, 1073 (1995)
6. C.L. Foden, N. Rando, A. van Dordrecht, A. Peacock, J. Lumley, C. Pereira, Phys. Rev. B **47**, 3316 (1993)
7. S. Friedrich, M.F. Cunningham, M. Frank, S.E. Labov, A.T. Barfknecht, S.P. Cramer, Nucl. Instr. Methods A **444**, 151 (2000)
8. G. Brammertz, A. Poelaert, A.A. Golubov, P. Verhoeve, A. Peacock, H. Rogalla, J. Appl. Phys. **90**, 355 (2001)
9. A.A. Golubov, M.Y. Kupriyanov, Sov. Microelectron. **14**, 428 (1985). (in Russian)
10. A.A. Golubov, M.Y. Kupriyanov, J. Low Temp. Phys. **70**, 83 (1988)
11. A. Barone, G. Paterno, *Physics and Applications of the Josephson Effect* (Wiley, New York, 1982)
12. V.A. Andrianov, M.G. Kozin, P.N. Dmitriev, V.P. Koshelets, I.L. Romashkina, S.A. Sergeev, AIP Conf. Proc. **605**, 161 (2002)